

Full Length Research Paper

Al-compositional variation in ophiolitic chromitites from the south Eastern Desert of Egypt: Petrogenetic implications

Mohamed M. Hamdy^{1*} and El-Metwally M. Lebda²

¹Geology Department, Faculty of Science, Tanta University, Tanta 31527, Egypt.

²Geology Department, Faculty of Science, Kafrelsheikh University, Kafrelsheikh, Egypt.

Accepted 11 July, 2011

Podiform chromitite bodies of variable sizes are hosted in the serpentinized ophiolitic dunite-harzburgite of the Arabian Nubian Shield in Arais (AR) and Malo Grim (MG) areas in the southern Eastern Desert of Egypt. The composition of chromian spinel in most of the studied chromitite samples has not changed significantly from its magmatic composition. However, the fractured and disseminated-textured ores were slightly metamorphosed under the lower greenschist facies (AR) to the transitional greenschist–amphibolite facies (MG). Alteration is recorded in individual chromite grains in the form of optical and chemical zoning. Core to rim chemical trends are expressed by MgO- and Al₂O₃- decrease, mainly compensated by FeO and Cr₂O₃ increases. The unaltered chromian spinel in these bodies displays a large range of Al estimating Cr# (Cr/Cr + Al) atomic ratio from 0.57 to 0.89. In AR chromitite, the Al-richer chromite interstitially occurs within the Al-poorer one, whereas in MG chromitite the variation of Al is between massifs. The calculated compositions of melts in equilibrium with chromian spinel of Al-richer and Al-poorer chromites are island arc low-Ti tholeiites and boninites, respectively. The formation of high-Cr chromitites is interpreted as a result of the extensive reaction of harzburgite with migrating island arc tholeiite melts of boninitic affinity. Melt–rock reaction produced boninitic melts and porous dunitic channels in which the mixing/mingling of melts promoted crystallization of monomineralic high-Cr chromian spinel. The presence of Al-richer chromite interstitially in the Al-poorer chromite in the AR ore was most probably due to metasomatism by Al-rich melts, which may be related to the intrusion of the Al-rich websterite. In MG, on the other hand, the wide distribution of Al in chromitites in small district most probably reflects temporal and/or spatial variations in the types of melt (boninitic and tholeiitic) that were generated from, and emplaced in, subarc mantle domains in a supra-subduction zone environment.

Key words: Al-compositional variation, podiform chromitite, mineral chemistry, alteration, tholeiitic and boninitic melts, supra-subduction zone, south Eastern Desert of Egypt.

INTRODUCTION

Cr-spinel [(Mg, Fe²⁺) (Cr, Al, Fe³⁺)₂O₄] is a common accessory mineral in ultramafic and mafic rocks. It also forms monomineralic bodies (chromitites) of economic value which are found scattered in the mantle section of ophiolite complexes worldwide. Chromitites in the Eastern Desert of Egypt are widespread in the ophiolitic ultramafic rocks of the Arabian Nubian Shield (ANS), but

are concentrated mainly in its southern part. The ANS ophiolites are metamorphosed. A high degree of metamorphism sometimes hinders the identification of the primary lithology of these ultramafic rocks. It has been demonstrated that the chromite can provide useful information about the petrological nature of its mantle source and geodynamics (Arai and Yurimoto, 1994; Zhou and Robinson, 1997; Barnes and Roeder, 2001; Proenza et al., 2008; Hamdy et al., 2011) because it preserves geochemical signatures of its source magmas. Furthermore, composition of chromian spinel is used as a petrogenetic indicator of the metamorphic processes that

*Corresponding author. E-mail: mhamdyeg@yahoo.ca, mohamed.hamdy@science.tanta.edu.eg. Fax: +2 040 3305804.

affected the ophiolitic chromitites (González-Jiménez et al., 2009). However, compositional variability is very common in accessory chromites in ultramafic and mafic rocks (Suja and Streider, 1996; Proenza et al., 2004; Garuti et al., 2007) and may arise due to sub-solidus re-equilibration of the chromite with surrounding silicate minerals and interstitial melt (Scowen et al., 1991; Rollinson, 1995). In contrast, massive chromitite successfully retains the pristine composition (Mondal et al., 2006), thus it is always a petrogenetic and tectonic indicator.

The genesis of podiform chromitite is one of the important igneous processes within the upper mantle. In ophiolites, podiform chromitites of magmatic origin occur in depleted peridotites left after extraction of basaltic magmas (Lago et al., 1982; Roberts and Neary, 1993). The chromitites are thought to mark zones of extensive melt/rock interaction (Zhou et al., 1996, 2001). In such settings, chromian spinel displays a large range of composition, reflecting its primary magmatic origin (Zhou and Robinson, 1994; Arai, 1997; González-Jiménez et al., 2011).

Ultramafic rocks from Arais (AR) and Malo Grim (MG) in the South Eastern Desert of Egypt are composed mainly of ophiolitic serpentized harzburgites. Serpentized non-ophiolitic olivine websterite occurs also within the AR ultramafic rocks (Hamdy and Lebda, 2007). The AR non-ophiolitic websterites are significantly varied in their compositions among Al-rich to Al-poor (Hamdy, unpublished). Based on the estimated O-H isotopic compositions of serpentization fluids and temperatures of metamorphism, Hamdy and Lebda (2007) proposed that the AR and MG peridotite rocks subjected to serpentization by continental metamorphic and/or hydrothermal fluids taking place mostly after their obduction. The temperature of the water that infiltrated the MG rocks was higher than that infiltrated the AR-rocks.

The obducted ophiolitic ultramafic rocks (particularly the MG peridotites) underwent progressive metamorphism (regional) causing alteration of aluminian chromite to intermediate Fe³⁺-rich aluminian chromite, ferritchromite zone and Cr-magnetite outer zone and formation of talc and anthophyllite. This transferred the peridotites from the lower greenschist facies to the transitional greenschist-amphibolite facies (MG) at T=500–550°C. On the other hand, the AR non-ophiolitic olivine websterite was probably serpentized (T < 500°C) before its emplacement in the obducted ophiolitic peridotite rocks, most probably by a mixture of an oceanic water released from the subducted oceanic crust and a magmatic water from the continental mantle wedge. By progressive cooling, the rock suffered retrograde metamorphism in the lower greenschist to the greenschist facies. Chromitite bodies of variable size occur within the mantle section of the AR and MG ophiolite ultramafic massifs. These chromitites are of

particular interest because they are one of the few examples where aluminum content varies widely within the same ultramafic massif, over a short distance, and even in the same sample. Here, we discuss the chromian spinel composition and petrography of these chromitites supplying a platform for addressing the origin of these chromitites, their relationships with the host ultramafic rocks, their tectonic setting and their broader significance with respect to the spatial co-existence of varied Al-containing chromitites. In addition, an assessment of the potential effect of sub-solidus element re-distribution due to alteration and metamorphism is required.

GEOLOGIC SETTING

Serpentinized mantle peridotite slices are common in the ANS of the Eastern Desert of Egypt. These rocks are commonly regarded as part of the widely distributed dismembered ophiolite sequence. They were formed during the arc stage (~870 to 690 Ma; Azer and Khalil, 2005) in supra-subduction zone (SSZ) setting (Abu El Ela, 1996; Stern et al., 2004; El Gaby, 2005; Azer and Stern, 2007), due to seafloor spreading (Pearce, 2003; Stern et al., 2004) that opened the Mozambique Ocean. The SSZ ophiolites from the ANS were formed at spreading centers in forearc (Shervais et al., 2004; Azer and Stern, 2007; Hamdy et al., 2011) or back-arc (Ahmed et al., 2001; El Gaby, 2005) convergent margin. Neoproterozoic crustal growth of the ANS was accomplished mostly through the accretion of the island arc to the continental margins, as the Mozambique Ocean was closed during the Pan-African orogenic event (650 to 620 Ma, Kröner et al., 1987). Subduction was active while the process of ophiolitic overthrusting was operative along the thrust planes (Kröner et al., 1987; Stern, 1994). Petrology of some rock units in the ANS of the Eastern Desert proves the recycling of the subducted slab and its role in the evolution of Neoproterozoic rocks (Eliwa et al., 2006; Hamdy et al., 2011).

The AR area lies between latitudes 23° 31' 20" and 23° 34' 10" N and longitudes 34° 49' 40" and 34° 54' 45" E, and the MG area lies between latitudes 22° 17' 30" and 22° 21' N and longitudes 36° 09' 30" and 36° 17' E. The AR area (Figure 1A) is reached at 65 km from Bernice on the Bernice-Shalatin road, and then westward along W. Marafai to Bir El-Gahliya and then for further 33 km along W. Bitan. The MG area, on the other hand, (Figure 1B) can be reached at 150 km from Shalatin on the Shalatin-Halaib road, then going for 50 km to the west through W. Yoider. The two study areas include large slices of the ophiolitic serpentized peridotites and metagabbros and island-arc volcanoclastic metasediments, in addition to pillow lavas and pelagic sediments in MG (Abu El Laban, 2002). The ophiolitic peridotites occur also as small isolated sheets or slabs tectonically mixed with the island arc rock assemblage, where they thrust over the island

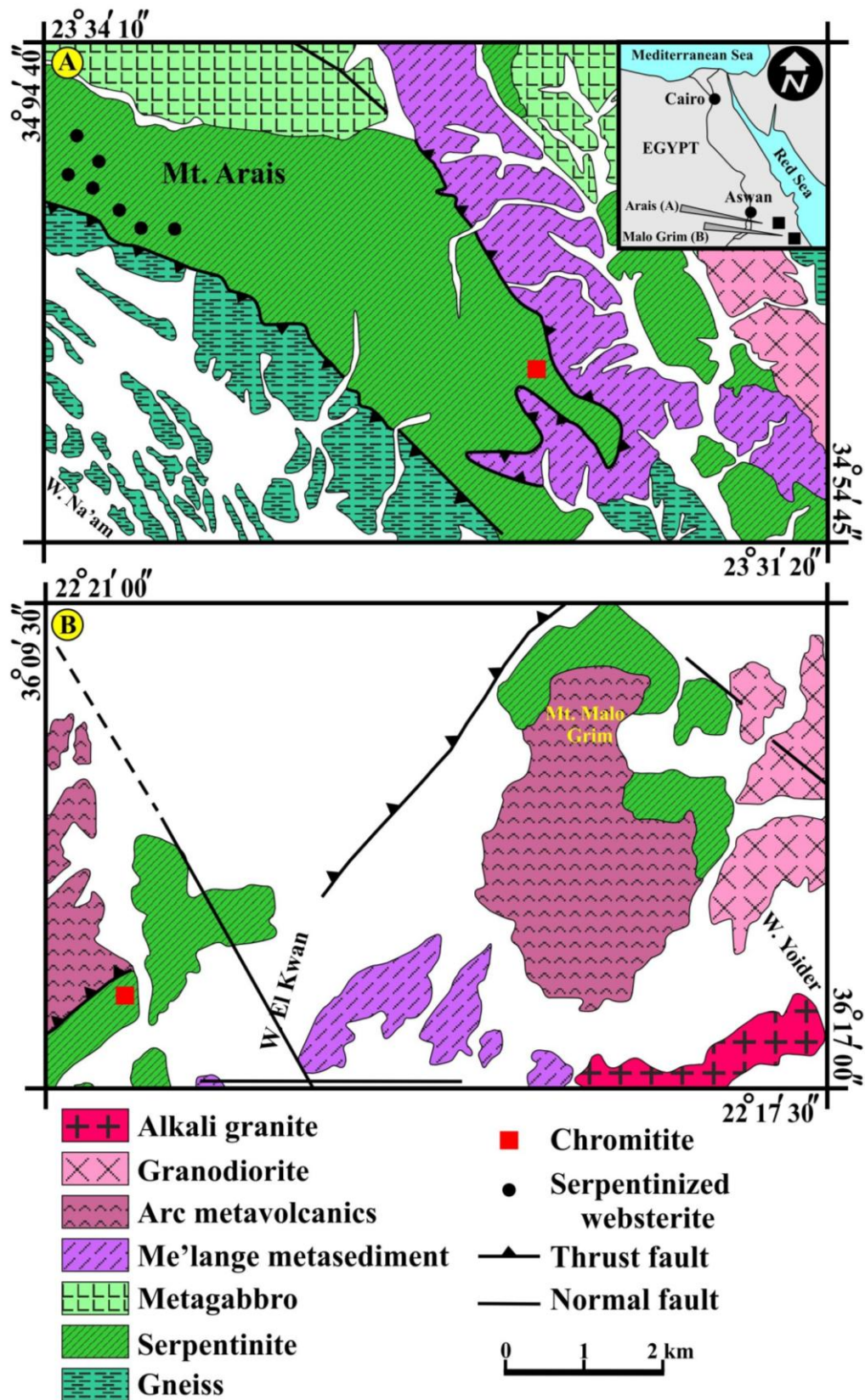


Figure 1. Geological maps of (A) Arais (after Ghoneim et al., 2002; sites of the serpentinized websterite are from Hamdy and Lebda, 2007) and (B) Malo Grim (after Abu El Laban, 2002) showing localities of the chromitite bodies.

arc volcanics and volcanoclastic metasediments along a major NW–SE trending thrust fault, forming an ophiolitic mélange (Ghoneim et al., 2002). Toward the top of the mantle tectonites, the peridotite contains increasing amounts of dunite, gabbro sills, and chromitite; all forming elongated pseudotabular bodies in parallel to the foliation of the host peridotite, as well as discordant dikes of gabbro and pegmatitic gabbro. The ultramafic rocks are usually sheared along their contacts with the mélange matrix, where veined mineralizations such as magnesite are abundant (Hamdy, 2007). All these rocks are intruded by syn-collision and post-collision granites.

Chromitite deposits occur mainly as lenticular bodies of variable dimensions up to 25 m length × 6 m width, trending ENE-WSW. According to the classification of Cassard et al. (1981), the pods appear to be concordant to sub-concordant with the host rocks. The thick pods are abundant in serpentinites that are mostly derived from dunite. The micro-lenses and thin planar segregations occur in the serpentinitized peridotite. Gradual contacts between massive ore and serpentinitized dunite over a meter-range are frequently observed. A typical contact shows gradation from fine-grained disseminated chromite in the dunite through nodular, to massive coarse-grained chromite ore. The massive chromitite is the most abundant in Arais area.

PETROGRAPHY

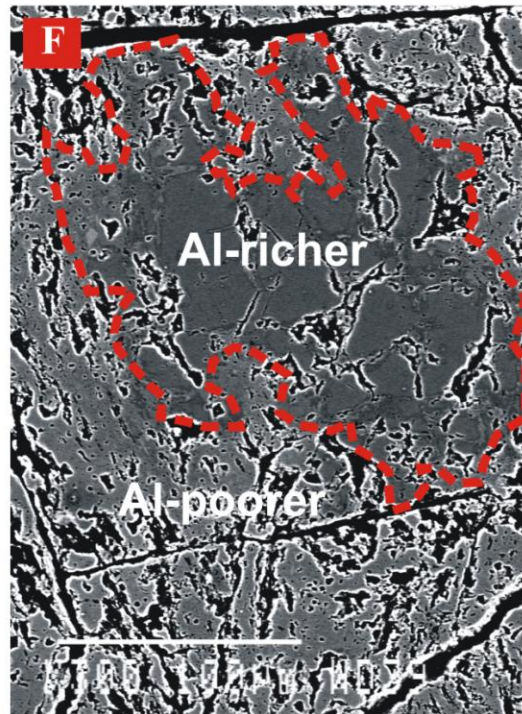
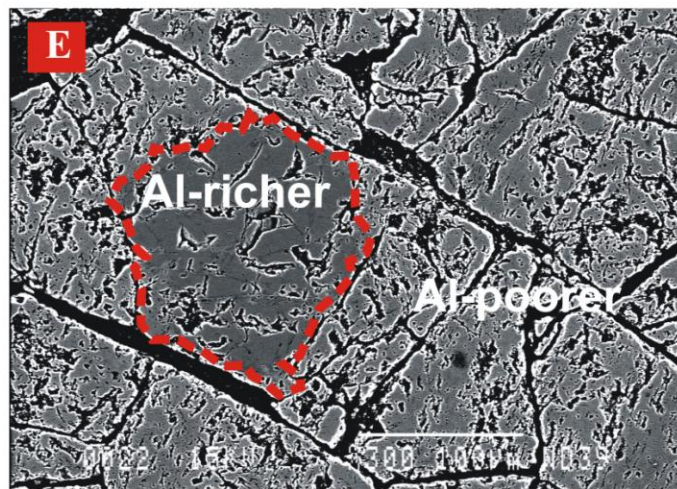
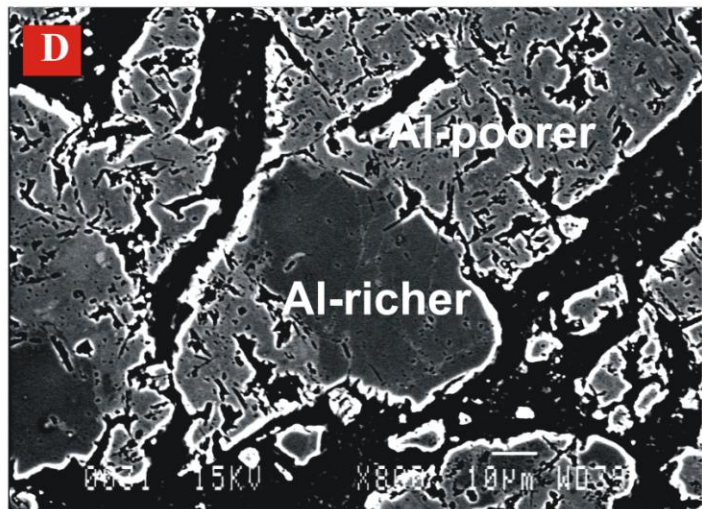
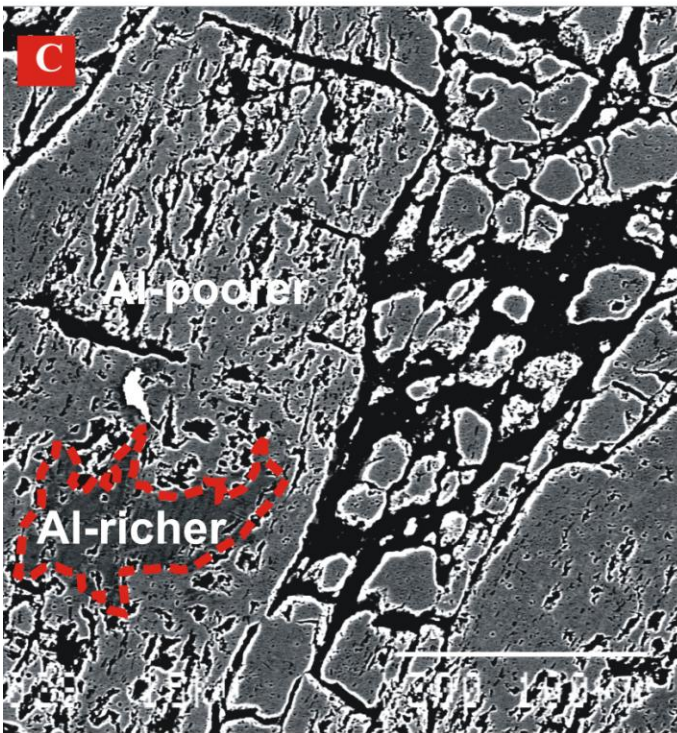
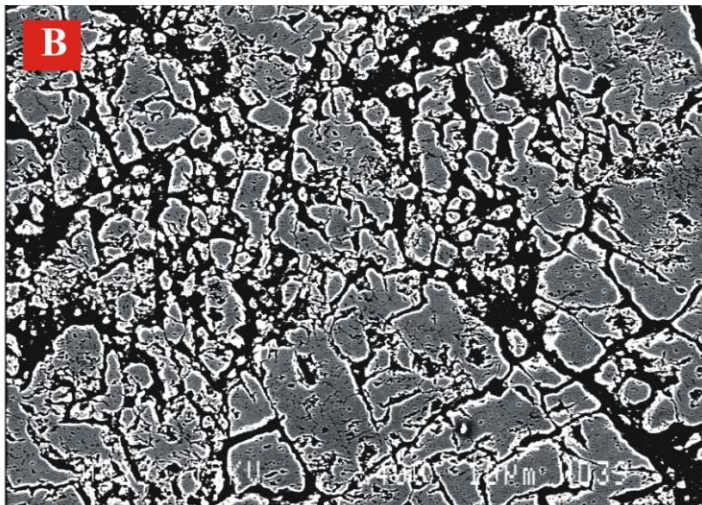
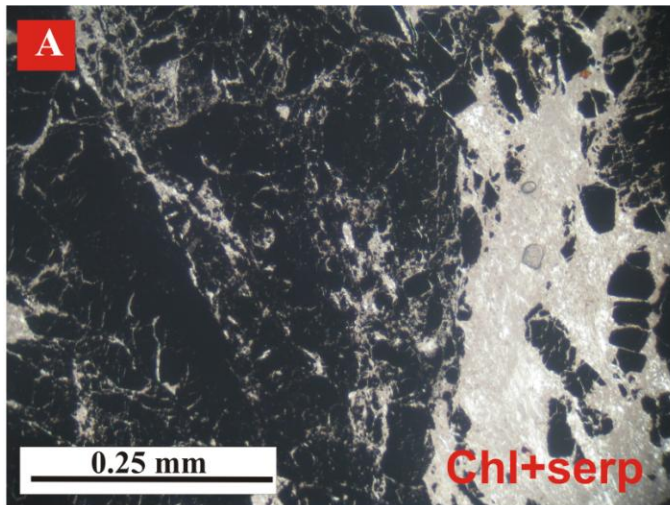
The textures of the chromitites have been investigated by reflected light and electron microscopy. Arais and Malo Grim chromitites display massive, lobate, brecciated and disseminated textures (Figure 2). The chromitites are commonly massive in the AR ore, whereas they are more fractured and mylonitized in the MG ore. Few chromite crystals are homogeneous and most are characterized by the presence of two or three optically different, that is, dark and light colored, phases. However, the heterogeneity of composition in chromite grains is represented by two types. The first type of compositional heterogeneity is found in massive-textured ores representing the presence of irregular zones corresponding to Al-rich chromite interstitially occurs within the Al-poorer chromite (Figure 2C to G). This grain-scale variation of Al is more abundant in the AR chromitite. However, the variation of Al in MG chromitite is observed among ore bodies. The second type of heterogeneity in chromite is represented by compositional zoning of the grains. This compositional zoning is more abundant in the brecciated and disseminated ores. The central part or core of the grain is darker than the outer rim which is lighter gray in color and has a higher reflectance. The central part is identified as remnant, unaltered chromite; the inner rim is of ferritchromite, whereas the outer rim is identified as

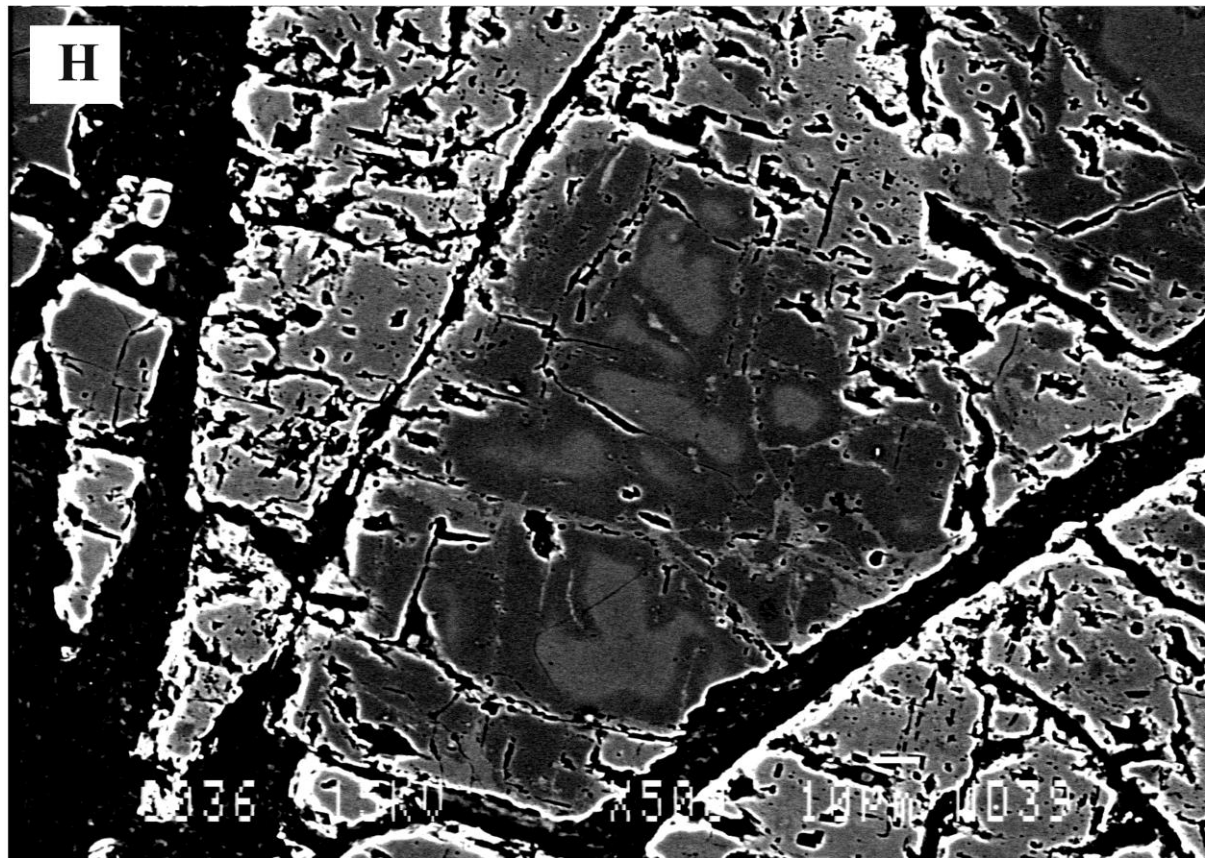
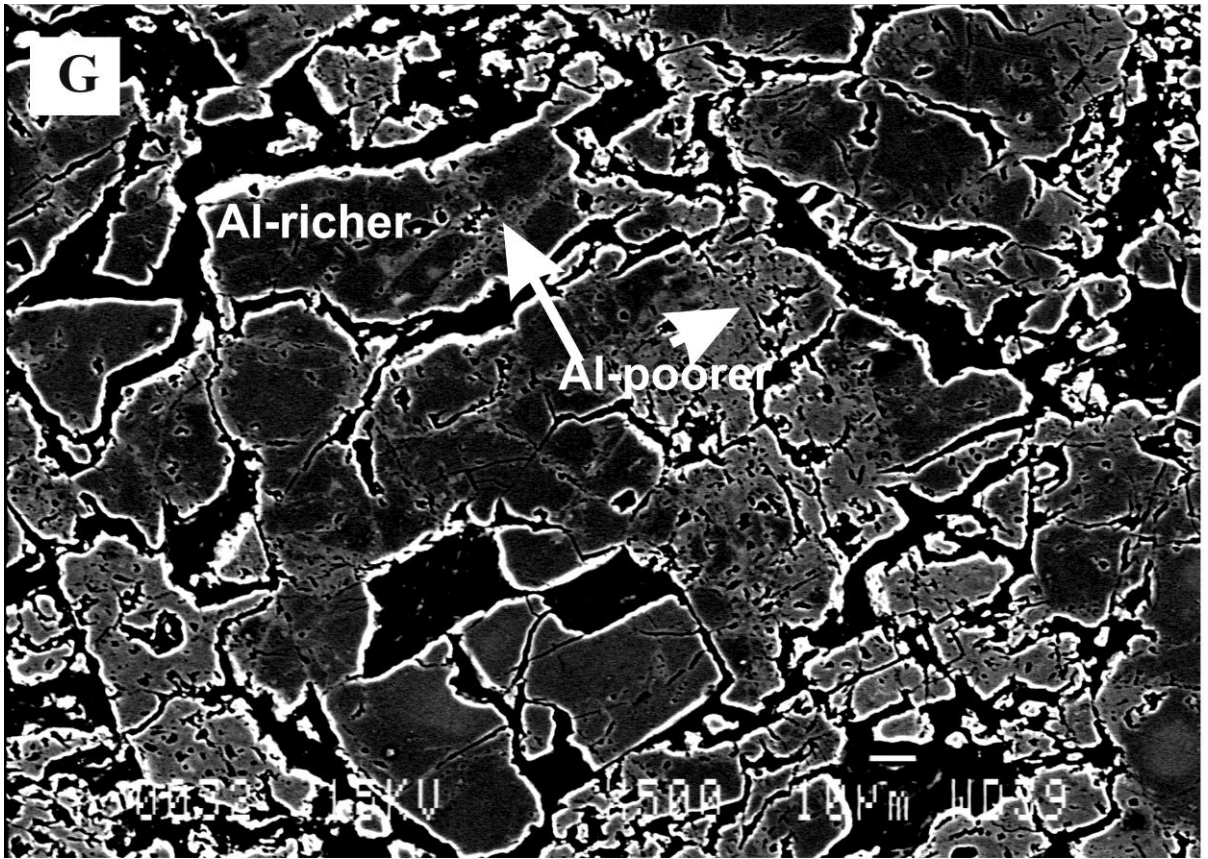
magnetite. The outer rim has highly irregular contacts with a surrounding chlorite. Occasionally, accessory chromite and chromite from the extensively altered massive chromitite show reversed zones, where the central part is lighter (Cr-rich) (Figure 2H and I). Magnetite occurs also along the fractures within the grains, and, is rare in occurrence compared to ferritchromite. The degree of alteration varies within a single body, depending on the size of the ore body and on the chromite/silicate ratio. Thus, massive chromitite are less altered than mid-sized and small ore bodies. Likewise, chromite from disseminated chromitites displays higher degrees of alteration than chromite from semi-massive and massive chromitites. As a consequence, alteration increases from the inner to the outer parts of chromitite bodies. The outermost altered zones often develop a porous texture containing abundant inclusions of secondary silicates such as serpentine or mostly chlorite.

No primary silicate minerals are preserved in the matrix of the chromitites in the studied samples. The fracture network and the matrix are composed mainly of chlorite, carbonates, talc, serpentine and magnetite. In massive chromitites, chlorite is the only gangue mineral constituting ~ 7 vol%, whereas it is mixed with serpentine in the disseminated one. Serpentine is also found as inclusions in altered and/or disrupted chromite grains. Primary silicate inclusions were also not recorded in the studied chromitites. However, primary silicates (olivine, clinopyroxene, amphibole and phlogopite) are reported in other chromitites, such as those of Wadi El-Zarka and Wadi Um Huitate areas (Saleh, 2006). Primary hydrous mineral inclusions are very common in chrome spinel of Phanerozoic ophiolite complexes and layered intrusions as well (Johan et al., 1983; McElduff and Stumpfl, 1991).

MINERAL CHEMISTRY

Quantitative chemical analysis of minerals (EMPA) was carried out at the Institute of Geological Sciences (IGS) of the Polish Academy of Sciences (PAS) and at the Faculty of Geology, University of Warsaw (UW). The EMPA at the IGS was carried out by JEOL-JXA-840A scanning electron microscope (SEM) equipped with Link Analytical AN-1000/855 energy dispersive X-ray spectrometer (EDS). The analytical conditions were 15 kV accelerating voltage and 35 nA beam current. The analyses at the UW, on the other hand, were performed by CAMECA SX 100 electron microprobe using wave dispersive X-ray spectrometer (WDS) with 15 kV accelerating voltage and 20 nA beam current. Synthetic silicate glasses as well as natural minerals were used as standards in both cases. Fe^{2+} - Fe^{3+} redistribution from electron microprobe analyses was made using the general equation of Droop (1987) for estimating Fe^{3+} .





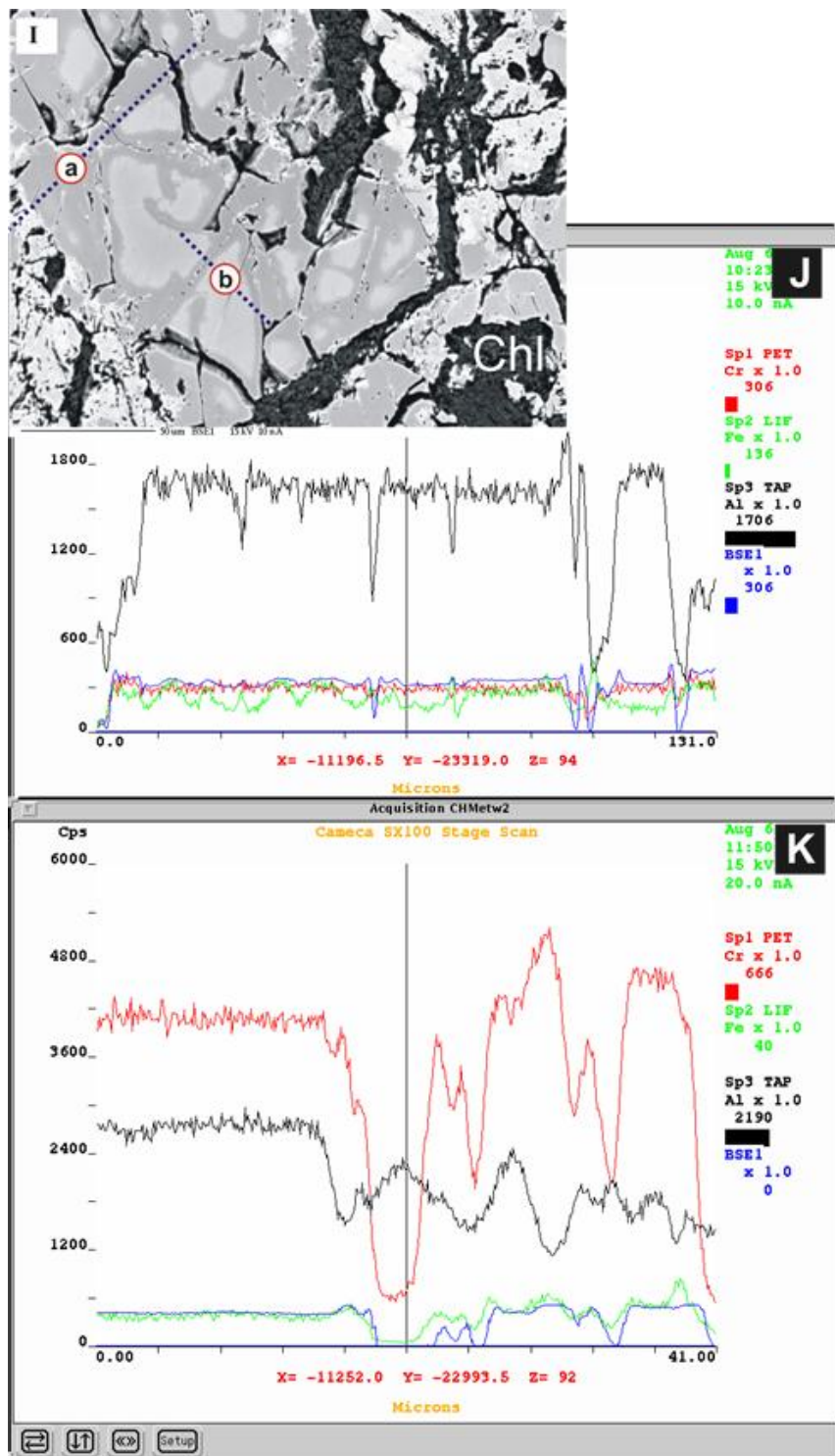


Figure 2. (A) Photomicrograph of the MG chromitite taken in transmitted light, showing fractured and disseminated-textured chromitites with interstitial chlorite and serpentine (chl+serp). (B) Back-scattered electron image (BSEI) of homogenous fractured chromite in the MG massive chromitite (sample # MG6). (C-G) BSEIs illustrate coexistence of the Al-rich and Al-poorer chromian spinels in AR chromitite. (H and I) BSEIs of zoning patterns of alteration in disseminated and fractured-textured chromitites from AR (sample# AR4) and MG (sample# MG7), respectively, showing a light central zone (Cr-rich), then a dark-coloured zone (Al-rich) and finally a light-coloured zone (rim) rich in Fe. (J and K) Chemical profiles of Cr, Fe and Al along sections (a) and (b) in microphotograph (I).

Table 1. Representative EMPA of Al-richer and Al-poorer chromites in AR and MG podiform chromitites.

	Al-richer chromite											
	Arais-AR						Malo Grim-MG					
	AR2-1-c	AR2-1-r	AR5-3-c	AR5-3-r	AR9-2-c	AR9-2-r	MG1-3-c	MG1-3-r	MG3-7-c	MG3-7-r	MG10-2-c	MG10-2-r
SiO ₂	0.03	0.00	0.16	0.09	0.07	0.23	0.12	0.02	0.03	0.00	0.02	0.01
TiO ₂	0.03	0.00	0.06	0.14	0.07	0.14	0.05	0.03	0.04	0.04	0.06	0.04
Al ₂ O ₃	21.44	20.94	18.88	20.24	23.02	21.14	20.03	18.61	17.97	19.46	18.56	21.47
FeO	18.99	17.05	11.25	13.21	21.53	15.07	8.82	18.90	19.39	19.56	19.53	19.91
Fe ₂ O ₃	0.64	1.34	2.97	1.05	0.14	1.31	3.56	4.60	4.46	5.15	4.92	6.23
Cr ₂ O ₃	52.55	51.89	55.06	53.89	48.77	48.74	54.56	47.10	47.26	44.83	45.99	41.86
MnO	0.01	0.06	0.00	0.00	0.00	0.00	0.15	0.18	0.40	0.32	0.32	0.28
MgO	6.61	8.45	11.86	11.57	5.49	12.78	13.23	9.73	9.43	9.47	9.22	9.67
CaO	0.002	0.005	0.001	0.00	0.001	0.01	0.01	0.00	0.00	0.00	0.00	0.02
NiO	0.04	0.00	0.00	0.08	0.31	0.00	0.00	0.01	0.035	0.18	0.07	0.12
ZnO	0.003	0.00	0.002	0.002	0.04	0.00	0.00	0.18	0.226	0.17	0.43	0.27
Total	100.3	99.74	100.2	100.3	99.44	99.42	100.5	99.35	99.39	99.36	99.29	100.0
	No. of cations on the basis of 32 oxygen atoms											
Si	0.008	0.00	0.04	0.022	0.018	0.057	0.029	0.004	0.009	0.000	0.006	0.003
Al	6.37	6.215	5.493	5.884	6.918	6.176	5.735	5.626	5.435	5.854	5.574	6.399
Ti	0.006	0.00	0.011	0.026	0.013	0.026	0.009	0.006	0.008	0.007	0.012	0.008
Fe ²⁺	4.007	3.593	2.324	2.727	4.594	3.127	1.792	4.059	4.189	4.219	4.252	4.211
Fe ³⁺	0.121	0.254	0.552	0.195	0.027	0.244	0.650	0.887	0.798	1.000	0.964	1.186
Cr	10.470	10.327	10.742	10.506	9.828	9.549	10.490	9.550	9.712	9.101	9.406	8.371
Mn	0.002	0.013	0.000	0.000	0.000	0.000	0.000	0.039	0.088	0.069	0.070	0.060
Mg	2.486	3.175	4.368	4.258	2.088	4.726	4.791	3.726	3.671	3.641	3.578	3.647
Ca	0.001	0.001	0.000	0.000	0.000	0.003	0.003	0.000	0.000	0.000	0.000	0.005
Ni	0.008	0.000	0.000	0.016	0.064	0.000	0.000	0.002	0.007	0.037	0.016	0.024
Zn	0.001	0.000	0.000	0.000	0.008	0.000	0.000	0.035	0.044	0.032	0.082	0.051
Mg#	0.38	0.47	0.65	0.61	0.31	0.60	0.73	0.48	0.47	0.46	0.46	0.46
Cr#	0.62	0.62	0.66	0.64	0.59	0.61	0.65	0.63	0.64	0.61	0.63	0.57
Fe ³⁺ #	0.007	0.015	0.033	0.012	0.002	0.015	0.039	0.055	0.050	0.063	0.060	0.074

Chromite

Compositions of the various phases have been established by microprobe analysis (Table 1). Most massive chromitite samples from Arias and

Malo Grim preserve primary chromite compositions. Their SiO₂ contents are invariably low (0.0 to 0.44 wt. % in AR and 0.00 to 0.28 wt. % in MG) and unrelated to the contents of the other major oxides. This igneous chromite

composition (Proenza et al., 2008) is also supported by the low Fe₂O₃ contents (0.14 to 2.97 wt. % in AR and 0.96 to 8.29 wt. % in MG) and high MgO contents (5.1 to 13.94 wt. % in AR and 0.28 to 13.23 in MG), which are characteristics of

Table 1 continues. Representative EMPA of Al-richer and Al-poorer chromites in AR and MG podiform chromitites.

Al-poorer chromite												
	Arais-AR						Malo Grim-MG					
	AR2-8-c	AR2-8-r	AR5-4-c	AR5-4-r	AR9-6-c	AR9-6-r	MG2-5-c	MG2-5-r	MG6-1-c	MG6-1-r	MG8-9-c	MG8-9-r
SiO ₂	0.14	0.07	0.05	0.18	0.20	0.44	0.02	0.07	0.13	0.28	0.04	0.05
TiO ₂	0.27	0.00	0.08	0.06	0.15	0.08	0.13	0.15	0.17	0.15	0.21	0.21
Al ₂ O ₃	13.11	9.58	14.67	8.39	10.25	13.54	10.43	8.02	8.82	10.88	11.91	4.68
FeO	16.92	16.94	16.15	11.58	10.03	22.68	25.71	13.14	26.47	25.46	11.28	29.09
Fe ₂ O ₃	0.95	1.62	0.56	2.15	2.89	0.93	1.24	1.08	5.62	5.89	0.96	8.29
Cr ₂ O ₃	58.98	63.54	58.76	63.81	64.49	55.81	59.31	64.55	55.17	53.98	62.44	56.58
MnO	0.00	0.00	0.00	0.00	0.00	0.00	0.01	0.34	0.37	0.41	0.17	0.15
MgO	9.01	7.79	10.29	12.42	13.94	5.10	2.61	12.68	2.34	2.88	11.91	0.28
CaO	0.01	0.00	0.01	0.02	0.01	0.00	0.00	0.00	0.02	0.01	0.00	0.04
NiO	0.09	0.49	0.00	0.66	0.09	0.37	0.00	0.61	0.021	0.00	0.45	0.06
ZnO	0.05	0.05	0.00	0.07	0.01	0.04	0.03	0.06	0.26	0.48	0.05	0.42
Total	99.53	100.08	100.57	99.34	102.05	98.99	99.49	100.71	99.37	100.41	99.42	99.85
No. of cations on the basis of 32 oxygen atoms												
Si	0.037	0.019	0.012	0.046	0.051	0.118	0.006	0.018	0.036	0.075	0.011	0.015
Al	4.037	2.997	4.256	2.531	3.024	4.285	3.393	2.457	2.915	3.506	3.615	1.596
Ti	0.026	0.000	0.015	0.012	0.028	0.016	0.027	0.029	0.035	0.03	0.041	0.046
Fe ²⁺	3.702	3.763	2.991	2.233	2.101	5.098	5.941	2.858	6.212	5.825	2.431	7.052
Fe ³⁺	0.187	0.324	0.115	0.461	0.544	0.188	0.258	0.211	1.185	1.212	0.186	1.808
Cr	12.18	13.329	11.433	12.906	12.759	11.845	12.94	13.259	12.228	11.662	12.708	12.95
Mn	0.000	0.000	0.000	0.000	0.000	0.000	0.002	0.075	0.088	0.095	0.050	0.037
Mg	3.513	3.085	3.779	4.742	5.206	2.043	1.075	4.917	0.977	1.175	4.576	0.118
Ca	0.003	0.000	0.003	0.005	0.001	0.000	0.000	0.000	0.005	0.002	0.001	0.011
Ni	0.019	0.105	0.000	0.136	0.018	0.081	0.000	0.128	0.005	0.000	0.093	0.015
Zn	0.008	0.007	0.000	0.014	0.001	0.008	0.006	0.012	0.053	0.097	0.010	0.091
Mg#	0.49	0.45	0.59	0.68	0.71	0.29	0.15	0.63	0.14	0.17	0.65	0.02
Cr#	0.75	0.82	0.73	0.81	0.81	0.73	0.79	0.84	0.81	0.77	0.78	0.89
Fe ³⁺ #	0.011	0.019	0.007	0.029	0.033	0.012	0.016	0.013	0.073	0.074	0.011	0.111

c, core; r, rim; Mg# = Mg/(Mg + Fe²⁺); Cr# = Cr/(Cr + Al); Fe³⁺# = Fe³⁺/(Fe³⁺ + Cr + Al).

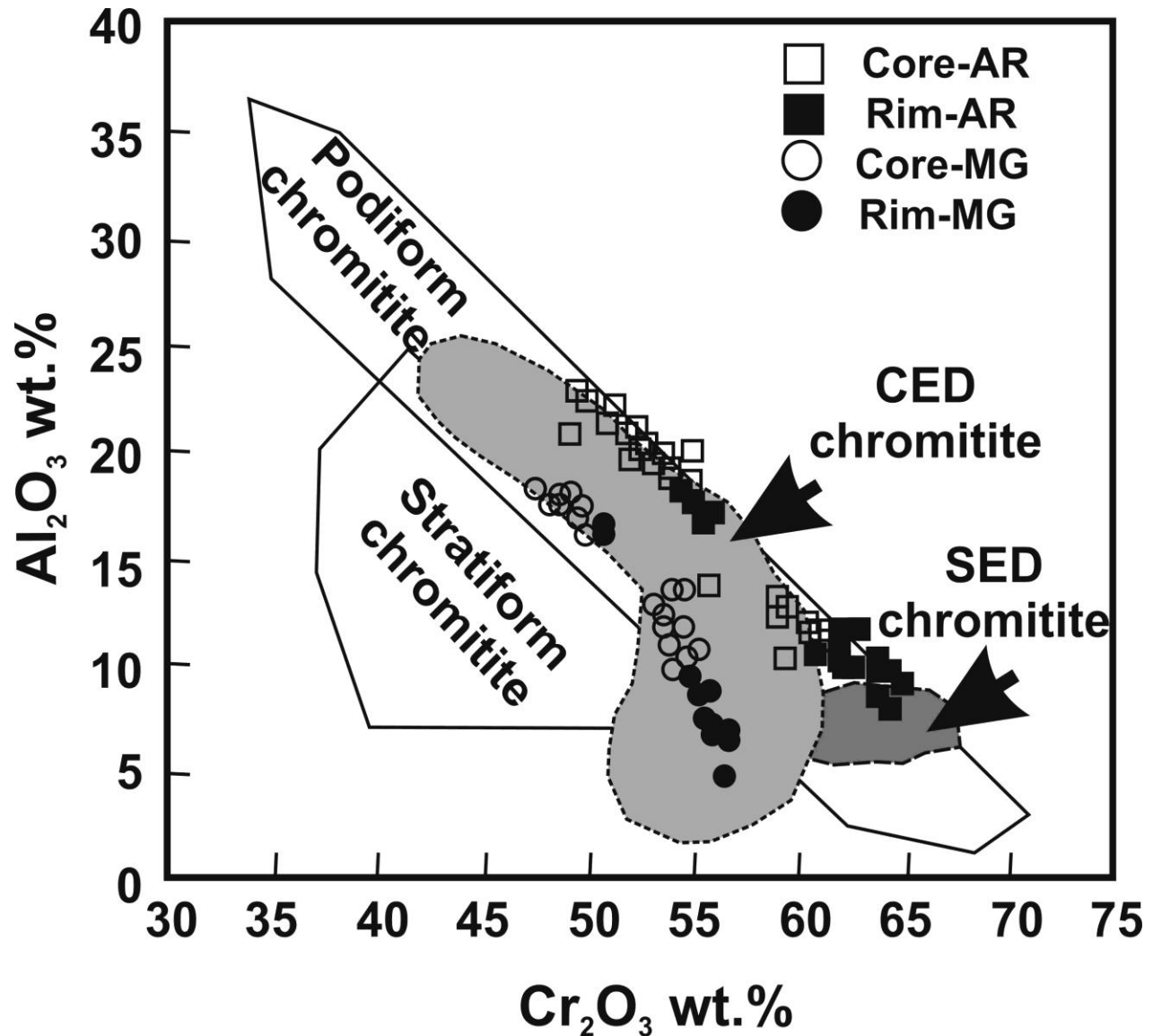


Figure 3. (a) Cr_2O_3 vs. Al_2O_3 plot of chromite compositions from the AR and MG chromitites. Compositional fields of podiform chromitites from the central (CED) and southern (SED) parts of the Eastern Desert of Egypt (Ahmed et al., 2001) are given for comparison. The podiform and stratiform fields are from Bonavia et al. (1993).

ophiolitic primary chromite (Proenza et al., 1999).

Although the massive chromitites are heterogeneous in composition at the grain scale (AR) and between ore bodies (MG), they are rarely zoned. The variation is mainly in Cr_2O_3 and Al_2O_3 contents. These contents vary from 48.74 to 64.49 wt.% and from 8.39 to 23.02 wt.% in AR ore, and from 41.86 to 64.55 wt.% and from 4.68 to 21.47 wt.% in MG ore. These wide ranges of Al and Cr estimate $\text{Cr}\#$ [$\text{Cr} / (\text{Cr} + \text{Al})$, cation ratio] varying from 0.59 to 0.82 in AR and 0.57 to 0.89 in MG. The $\text{Mg}\#$ [$\text{Mg} / (\text{Mg} + \text{Fe}^{2+})$] varies widely with the Al-Cr variation from 0.29 to 0.71 and from 0.02 to 0.73 in AR and MG, respectively. These primary chromite compositions correspond to Al-rich ($\text{Cr}\# \leq 0.6$) and Cr-rich chromites

($\text{Cr}\# > 0.6$) (Proenza et al., 2008). On the plots of Cr_2O_3 vs. Al_2O_3 (Bonavia et al., 1993), both AR and MG chromitite bodies have primitive chromite compositions within the range defined by ophiolitic chromitites (Figure 3). The $\text{Fe}^{3+}\#$ [$\text{Fe}^{3+} / (\text{Fe}^{3+} + \text{Cr} + \text{Al})$, cation ratio] is between 0.002 and 0.033 and between 0.011 and 0.11, in AR and MG chromitites, respectively. The TiO_2 contents are low (0.00 to 0.27 wt.% and 0.03 to 0.21 wt.%). These compositions are consistent with the compositions of podiform chromitites from central and southern parts of the Eastern Desert (Ahmed et al., 2001). The MG chromite shows enrichment in MnO (up to 0.41 wt.%) compared to the AR chromite (0.00-0.06 wt.%). NiO (≤ 0.66 wt.%) is very low. In contrast to the

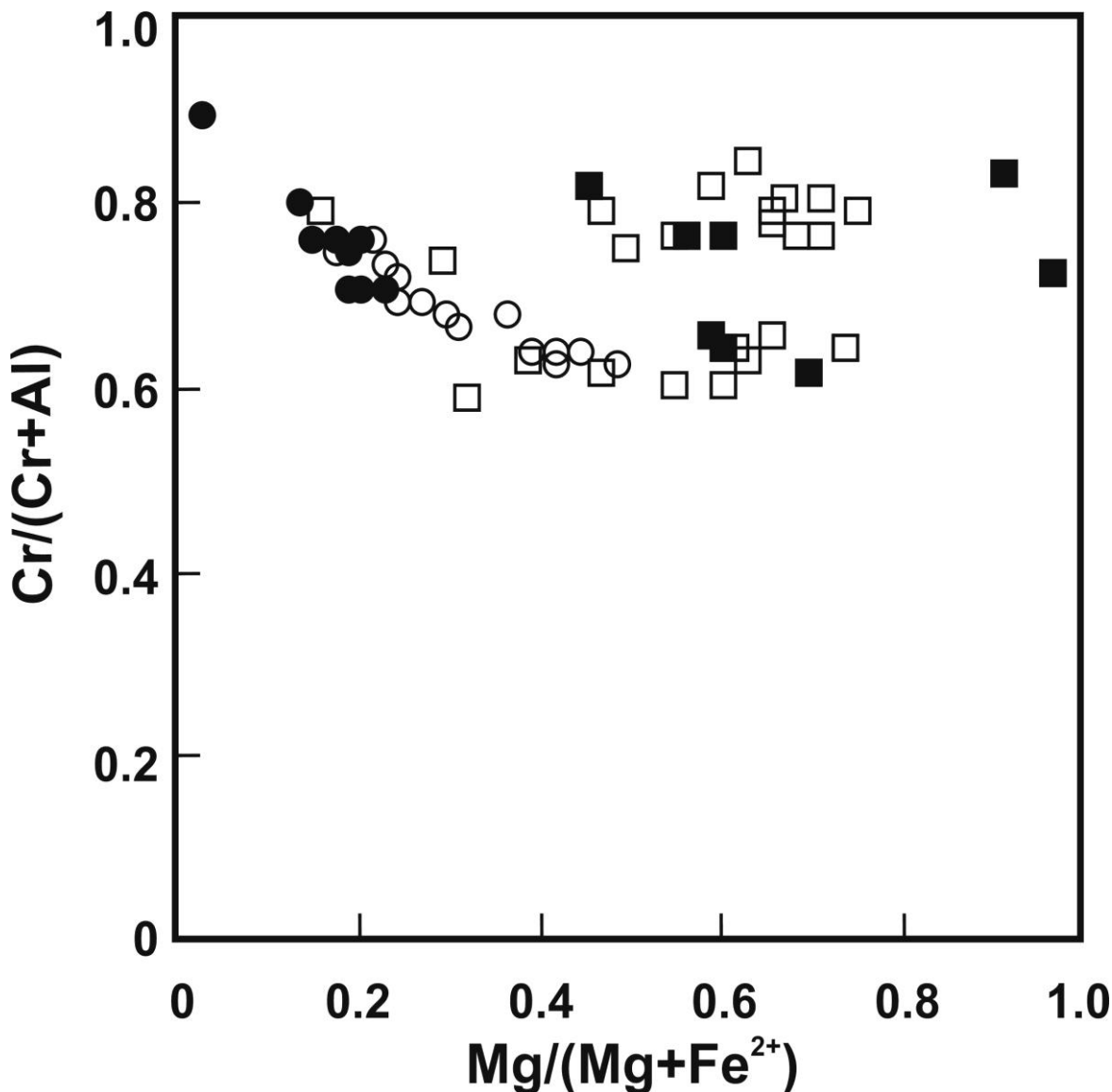


Figure 4. Variation of Cr-ratio plotted against the Mg-ratio in chromitite; MG chromite compositions refer to alteration trend, increasing Cr-ratio is due to loss of Al; AR chromite refers to decreasing magnesium ratio indicating fractional crystallization trend between different varieties of chromitite (Al-richer and Al-poorer). Symbols as in Figure 3.

massive-textured chromitites, the brecciated and the disseminated-textured ores are compositionally zoned. The smaller grains are compositionally more heterogeneous compared with the larger grains. This is well observed in the MG chromitite. Cr₂O₃ and MgO (high average atomic number: light) show enrichment in the core and progressive loss far from the core (lower average atomic number: dark) and sometimes re-enrichment toward the rim (Figure 2H and I). Al₂O₃ and FeO show complementary patterns of distribution with Cr₂O₃ and MgO (Figure 2J and K). Core to rim, Fe³⁺ enrichment is mainly observed in MG chromitite. This irregular and heterogeneous nature of variation is

definitely related to low temperature hydrothermal alteration (Mukherjee et al., 2010).

The primary compositional variation in the AR chromitite along the Mg/(Mg+Fe²⁺) axis in two ranges of Cr/(Cr+Al) ratios (0.59 to 0.66 and 0.73 to 0.82) indicates a fractional crystallization trend (Figure 4) (Mukherjee et al., 2010). In contrast, the MG chromitite samples exhibit an alteration trend due to Al-loss. In the Cr–Al–Fe³⁺ ternary diagram (Figure 5), two distinct compositional characters are recognized for the studied chromite; (1) chemical variation along the Cr–Al side by the AR chromite cores and rims in the mantle chromitite field of Arai and Yurimoto (1994) and (2) chemical variation

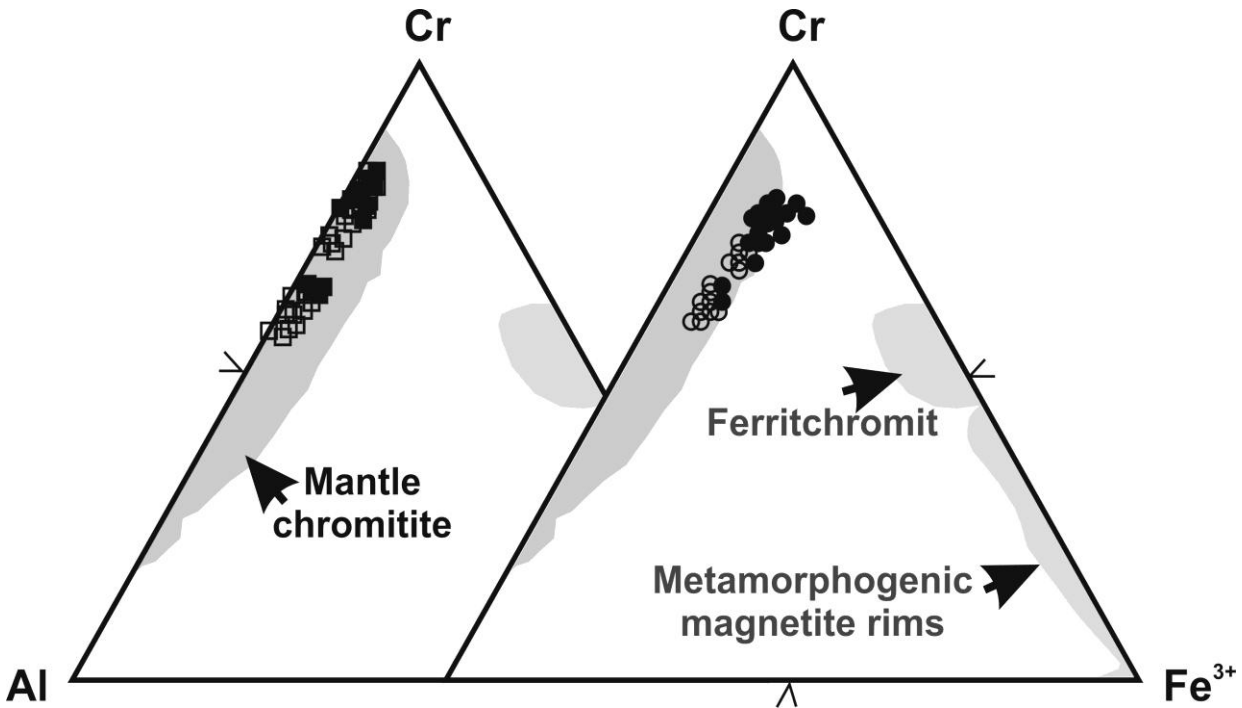


Figure 5. Cr–Al–Fe³⁺ variation of chromite; fields of mantle chromitite (Arai and Yurimoto, 1994), ferritchromit and metamorphogenic magnetite (Barnes and Roeder, 2001) are given for comparison. Symbols as in Figure 3.

along the Cr–Al side by the MG chromite cores in the mantle chromitite field, with increasing Fe³⁺ content in their rims outside the mantle field. However, rims of MG chromites do not fall within either the ferritchromit field or the metamorphogenic magnetite rim of Barnes and Roeder (2001). The composition of the MG chromitite is similar to the accessory chromites in their hosting serpentinites (Hamdy and Lebda, 2007).

The oxides of the minor elements show similar compositional trends with respect to fractional crystallization and alteration. The AR grains show restricted variation in composition and low concentration of TiO₂ and MnO over constant Fe³⁺ (Fe³⁺+Al+Cr, cation ratio) ratios (0.007 to 0.029). In MG chromites, increasing values of TiO₂ and MnO are observed with decreasing Mg-ratios and increasing Fe³⁺ ratios conform to the trend of alteration of Barnes (2000). No trend is observed for the minor elements other than for MnO and TiO₂. Overall, the element distribution patterns of chromian spinel indicate that the AR chromites represent pristine composition more than the MG chromites.

Interstitial silicates

Serpentine is found only in the matrix of the disseminated chromitites. It exhibits SiO₂ contents from 40.71 to 41.31 wt.%, and FeO from 2.08 to 2.12 wt.% (Table 2). Its contents of Al₂O₃ (2.34 to 2.91 wt.%) and Cr₂O₃ (2.67 to

2.97 wt.%) are relatively high compared to the serpentine from the hosting rocks (Hamdy and Lebda, 2007). The electron microprobe analyses of serpentine from chromitites probably can be influenced by their inhomogeneity and by limited resolution of the electron microprobe. Single analyses represent, in most cases, the bulk composition of two phases (serpentine and chlorite). Chlorite from the matrix of the chromitites shows SiO₂ contents between 25.27 and 34.09 wt.%, and low Fe contents (0.73 to 2.31 wt.% of FeO). The Fe/(Fe+Mg) ratio is normally below 0.05. The Si contents of chlorite (4.97 to 6.67 atoms per formula unit) classify them as sheridanite to clinocllore following the classification of Hey (1954). The Al₂O₃ contents of chlorites are generally lower than those of chlorite from the hosting ultramafic rocks (Hamdy and Lebda, 2007), most likely due to the entrance of Cr (up to 7.77 wt.% Cr₂O₃).

DISCUSSION

Alteration and metamorphism

Since reactions between Cr–Al spinel and silicates during cooling or metamorphism may produce a significant exchange of elements. Therefore, interpretations of the compositional variation in chromian spinel of the AR and MG chromitites in terms of primary magmatic processes first require an assessment of the potential effect of sub-

Table 2. Representative EMPA of interstitial silicates in AR and MG podiform chromitites.

	Chlorite				Serpentine	
	AR2-6	AR9-11	MG3-22	MG10-7	AR2-13	MG3-18
SiO ₂	32.52	25.27	34.09	28.29	40.71	41.31
TiO ₂	0.01	0.06	0.18	0.04	0.03	0.01
Al ₂ O ₃	14.47	25.63	13.14	20.41	2.91	2.34
Cr ₂ O ₃	4.75	3.27	1.23	7.77	2.97	2.67
FeO	0.73	1.05	0.81	2.31	2.12	2.08
MnO	0.00	0.00	0.10	0.00	0.12	0.09
MgO	32.73	27.86	32.97	28.73	39.24	39.17
CaO	0.02	0.18	0.00	0.05	0.02	0.06
Na ₂ O	0.00	0.00	0.08	0.00	0.01	0.00
K ₂ O	0.11	0.00	0.12	0.04	0.01	0.02
NiO	—	—	—	—	0.16	0.87
Total	85.33	83.31	82.72	87.65	88.3	88.62
Si	6.246	4.968	6.665	5.396	3.783	3.832
Al	3.276	5.941	3.028	4.589	0.318	0.256
Ti	0.002	0.009	0.026	0.006	0.002	0.001
Fe ²⁺	0.118	0.172	0.132	0.369	0.165	0.161
Cr	0.721	0.508	0.19	1.171	0.218	0.196
Mn	0.000	0.000	0.017	0.000	0.009	0.007
Mg	9.373	8.166	9.611	8.169	5.435	5.417
Ni					0.012	0.065
Ca	0.005	0.037	0.000	0.011	0.002	0.006
Na	0.000	0.000	0.029	0.000	0.002	0.000
K	0.026	0.000	0.032	0.011	0.001	0.002
O	28	28	28	28	14	14
Mg#	0.98	0.97	0.98	0.96		

—, not applicable; Mg# = Mg/(Mg + Fe²⁺).

solidus element re-distribution. As the secondary silicates (serpentine and chlorite) are the only occurring as inclusions or in the matrix of chromite, thus we should estimate the exchange of elements between chromite and these minerals, in terms of metamorphism. Estimated peak temperatures of the metamorphism in ophiolitic ultramafic rocks from AR and MG are between 176 and 550°C, corresponding to the lower greenschist to the transitional greenschist-amphibolite facies (Hamdy and Lebeda, 2007). As discussed before, the element distribution patterns of chromian spinel indicate that the AR chromitite represents more primitive composition and is slightly affected by the alteration compared to the MG chromitite. The alteration rims of chromite of MG chromitite have a chemical composition that provides evidence of an alteration event characterized by FeO enrichment and Cr# increase (caused by loss of Al₂O₃) with little or no variation in Fe₂O₃ content. According to Evans and Frost (1975) and Suita and Streider (1996), such chemical variation is typical of chromite altered under greenschist facies (200-400°C; Ernst, 1993) metamorphism. Formation of high-Cr, low-Fe³⁺ spinels

(depending on the chromite/silicate ratio) start to form, with a sharp compositional (miscibility) gap with the inner primary core, around the transitional greenschist–amphibolite facies to lower amphibolite facies metamorphism (Arai et al., 2006). Secondary Cr-rich chlorite (sheridanite to clinocllore) occurring as interstitial phase between altered chromite formed during the later regional metamorphism. Barnes (2000) inferred that the Mg# of the altered chromites varies from 0.4 to 0.7 for spinels altered under greenschist facies condition and is less than 0.35 for those altered in the amphibolite facies. At relatively high temperatures (> 400°C); the Mg- and Al-rich components of the primary chromite react with MgO- and SiO₂-rich fluids to produce chlorite (Kimball, 1990). The formation of chlorite through this reaction implies outward diffusion of Al and Mg from chromite, leaving a residual Fe²⁺-, Cr³⁺-enriched and Al-, Mg-depleted chromite. Consequently, the textural and compositional features of the secondary chromites match those of the transitional greenschist–amphibolite facies metamorphism. The chemical composition of the studied chromites, both cores and rims, are plotted on the

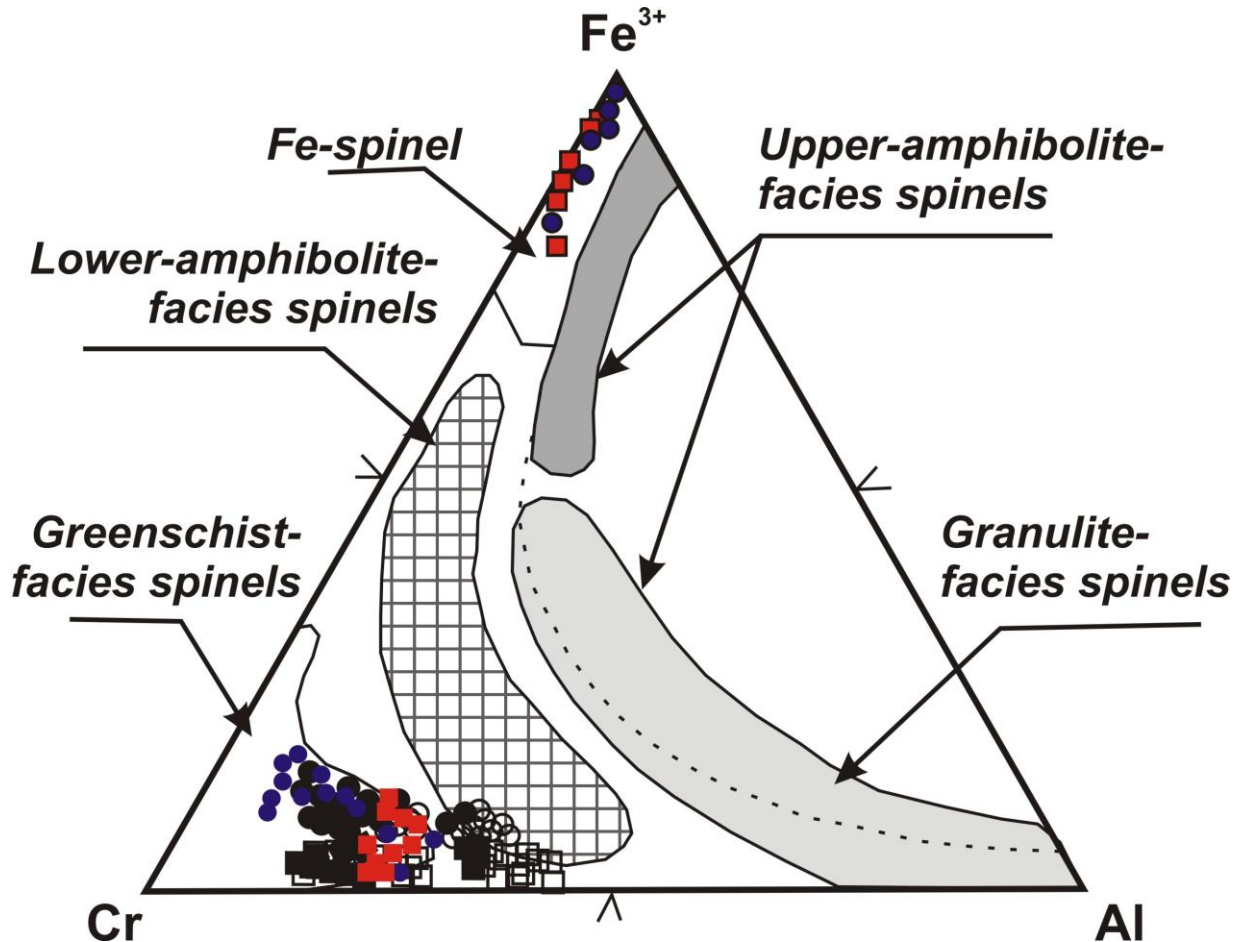


Figure 6. Cr–Al–Fe³⁺ triangular plot of the AR and MG chromites. The solvus curve (dashed line) and fields of different metamorphic facies for Cr-spinel phases are from Evans and Frost (1975), Suita and Streider (1996) and Barnes and Roeder (2001). Symbols as in Figure 3. Spinels in serpentinites from AR (red closed boxes) and MG (blue closed circles) (Hamdy and Lebda, 2007) are given for comparison.

triangular Fe³⁺–Cr–Al diagram (Figure 6), which shows the spinel compositional fields from different metamorphic facies (Evans and Frost, 1975; Frost, 1991; Suita and Streider, 1996; Barnes and Roeder, 2001). The compositions of AR chromitite cores and some of their rims lie on the Al–Cr line outside any field of metamorphic facies. On contrary, the compositions of chromite, cores and rims from the MG chromitites and some of the AR chromite rims lie in the field of chromian spinels from the greenschist facies and are between fields of greenschist facies and lower amphibolite facies, within the proposed solvus (miscibility gap) from prograde metamorphic rocks. This proves that the AR chromitite slightly was metamorphosed under lower greenschist facies, whereas the MG chromitite underwent stronger alteration under the transitional greenschist–amphibolite facies metamorphism. Furthermore, as the extent of the component exchange is strongly dependent on chromite/silicate ratio, the fact that almost all the chromitite bodies consist mainly of monomineralic

chromian spinel (that is, massive-textured ore), with only minor amounts of silicates present as inclusions, suggests that the composition of chromian spinel in most of the studied chromitite samples has not changed significantly from its high-temperature magmatic composition.

The parental melt of the chromitite: composition and tectonic setting

As the metamorphic modifications of chromite compositions were assessed, the primary magmatic compositional trends of the chromian spinel (particularly in AR chromitite) were not substantially disturbed since the magmatic stage. However, as we considered the alteration that might occur to the rims of these chromites, the cores of the chromian spinel can be used to obtain valuable information on the geochemical signature of the chromite parental magmas and the tectonic setting of

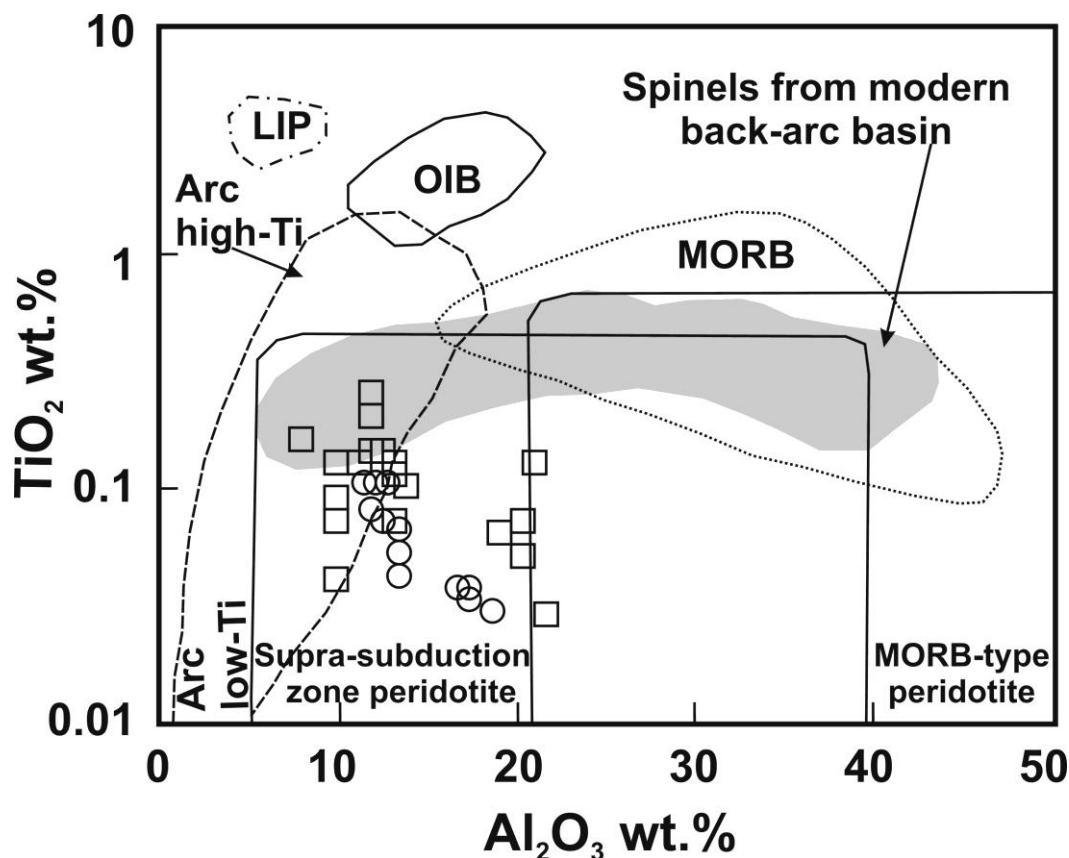


Figure 7. Primary chromite composition plotted on Al_2O_3 vs. TiO_2 tectonic discrimination diagram of Kamenetsky et al. (2001).

their genesis. The genesis of mantle-hosted ophiolitic chromitites is still debated, although they may have formed by melt-rock reaction (Arai and Abe, 1994; Arai and Yurimoto, 1994; Proenza et al., 1999). Rollinson (2005) argued that the compositional variations in ophiolitic chromitites are related to the process of a melt-rock reaction rather than different tectonic environment. In addition, the presence of water in the melt is thought to be necessary for the crystallization of ophiolitic chromite (Edwards et al., 2000). The tectonic setting for chromitite crystallization is a subject of dispute (Lago et al., 1982). However, experimental results in water-oversaturated basalts (Matveev and Ballhaus, 2002) suggest that ophiolitic chromitites would form only in the presence of primitive melts saturated in olivine–chromite and rich in water. Such conditions most likely occur in supra-subduction zone environments. By contrast, no ophiolitic chromitites are thought to form in mature spreading centers, such as mid-ocean ridges (Arai and Abe, 1994; Robinson et al., 1997; Schiano et al., 1997; Edwards et al., 2000).

Supra-subduction ophiolites could form either in forearcs during an incipient stage of subduction initiation or in back-arc basins. High Cr# of chromite from

serpentinites in the Eastern Desert of Egypt has been interpreted as formed in forearc basins rather than back-arc basins, which are relatively difficult to emplace (Stern et al., 2004; Azer and Stern, 2007; Hamdy et al., 2011). On the TiO_2 vs. Al_2O_3 tectonic discrimination diagram (Figure 7) of Kamenetsky et al. (2001), all primary chromites (cores) lie in the field of the supra-subduction zone; most of them in the Arc-low Ti field and some lie to the boundaries with the MORB and the modern back-arc basin.

The results of experimental crystallization studies (Roeder and Reynolds, 1991) suggest that chromite composition is controlled mainly by the composition and oxygen fugacity of the melt, and is only weakly dependent on temperature and pressure. The Cr/Al ratio of chromite in equilibrium with a given melt is controlled by the total concentration of Cr_2O_3 and Al_2O_3 in the melt, whereas the Cr content in chromite shows a negative correlation with the Al content in the melt.

In ophiolitic complexes, Al-rich chromitites tend to occur at the shallowest levels of the upper mantle, within the so-called Moho Transition Zone (Leblanc and Violette, 1983; Proenza et al., 1999). Al-rich chromitites are considered to form from tholeiitic melts (Zhou and

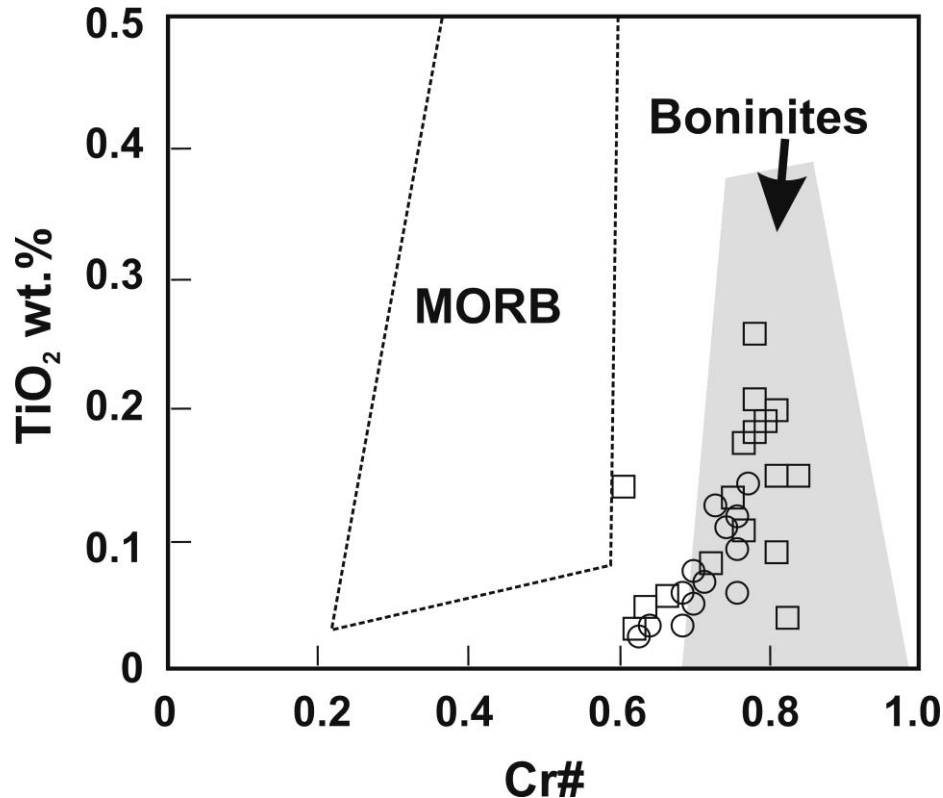


Figure 8. Primary chromite composition plotted on Cr# vs. TiO₂. Fields of MORB and boninite are from Dick and Bullen (1984) and Arai (1992).

Robinson, 1997). On the other hand, the high Cr-chromite is genetically linked to high-Mg andesite, boninite, or high-Mg arc tholeiitic (Zhou and Robinson, 1997; Abu El Ela and Farahat, 2010). On the TiO₂ vs. Cr# magma type discrimination diagram (Figure 8), most of chromites from AR and MG lie in the boninite field. Yet some analyses lie in between the MORB and boninite fields. We calculated the Al₂O₃ content of the parental melts in equilibrium with the AR and MG chromitite bodies using the equation proposed by Maurel and Maurel (1982) for spinel-liquid equilibrium at 1 bar where $(Al_2O_3)_{Sp} = 0.035(Al_2O_3)_{liquid}^{2.42}$. This equation is based on the observation that the Al₂O₃ (wt.%) in spinel is a function of Al₂O₃ (wt.%) in melt. The estimated melt composition have Al₂O₃ contents of 13.45 to 14.38 wt.% and 13.37 to 14.98 wt.% for the Al-richer chromites of AR and MG, respectively, and 9.44 to 11.7 wt.% and 9.82 to 10.71 wt.% for the Al-poorer chromites of AR and MG, respectively. The TiO₂ content of the melt is obtained from the melt-TiO₂ versus chromite-TiO₂ diagram of Kamenetsky et al. (2001). The estimated melt composition have TiO₂ contents of 0.09 to 0.6 wt.% and 0.02 to 0.18 wt.% for the Al-richer chromites of AR and MG, respectively, and 0.19 to 0.69 wt.% and 0.29 to 0.54 wt.% for the Al-poorer chromites of AR and MG, respectively. The Al₂O₃ and TiO₂ of the parental melt of

the Al-richer chromites compare with those of the low-Ti, high-Mg tholeiitic magma (Al₂O₃ = 11.4 to 16.4 wt.%: Augé, 1987), whereas those of the parental melt of the Al-poorer chromites compare with those of the boninitic magma (Al₂O₃ = 10.6 to 14.4 wt.%: Wilson, 1989). This is clearly different from the MORB magma (Al₂O₃ = ~15 wt.%: Wilson, 1989; Fryer et al., 1990). The likely low-Ti tholeiitic to boninitic affinity of the parental melt of the studied chromitites suggests formation in an arc-marginal basin setting.

The high Cr# in AR and MG chromitites (Al-poorer) implies a high degree of partial melting of depleted mantle of deep source (Rollinson, 2008; González-Jiménez et al., 2011). The formation of high-Cr chromitites is interpreted as a result of the extensive reaction of harzburgite with migrating island arc tholeiite melts of boninitic affinity. Melt-rock reaction produces boninitic melt and porous dunitic channels in which the mixing/mingling of melts promotes crystallization of monomineralic high-Cr chromian spinel (González-Jiménez et al., 2011). According to the melt-rock interaction model and despite the above mentioned controversy concerning the importance of water in the formation of chromitites, the Cr# of the spinel is controlled by both the degree of depletion of the mantle source, due to previous melting, and the degree of the second-stage

melting. The latter is presumably controlled mainly by the melt/rock ratio, together with temperature and compositions of the melt.

The Al-rich chromitite, on the other hand, is interpreted to be the result of chromite-forming, olivine dissolving melt/rock reactions produced when basalt melts migrated by porous flow through dunitic channels, and mixed with oxidized, volatile-rich melts in the supra-subduction mantle (Proenza et al., 1999, 2004, 2008). However, Al-enrichment might be caused by metasomatism with Al-rich melts (Grieco et al., 2004).

Coexistence of the Al-richer and Al-poorer chromites

The coexistence of high-Cr and high-Al chromitites is a common feature of many ophiolitic belts. The two chromitite varieties may occur in separated massifs (Proenza et al., 1999; Ahmed et al., 2001; Uysal et al., 2009) or less frequently interspersed within a single ultramafic massif containing variably depleted peridotites (Melcher et al., 1997; Proenza et al., 1999). A bimodal distribution and vertical zoning have been observed in some cases, with high-Al chromitites being located towards the petrological Moho and high-Cr chromitites in deeper parts of the mantle section (Ahmed and Arai, 2002; Rollinson, 2008). Although both of the AR and MG chromitites are characterized by having wide ranges of Al compositions, the origin of each ore is interpreted in a different model.

For the AR chromitites, textural feature such as the interstitial Al-richer chromite in the poorer one (grain-scale) is against the model of the progressive fractionation of parental melt, initially Cr-rich in SSZ and arc regions (Graham et al., 1996). The fractionation would produce a decreasing Cr and increasing Al outside the core, which is not our case. It is interpreted that the grain-scale Al-variation in AR chromitite is mostly the result of metasomatism by Al-rich melt (Peighambari et al., 2011) of low-Ti tholeiitic affinity. Presence of Al-rich non-ophiolitic (intrusive-affiliated) websterites within the AR ultramafics (Hamdy and Lebda, 2007) and their role in enrichment of the AR peridotites (Hamdy, unpublished) may support the idea of Al-metasomatism in AR chromitite. In this case, metasomatism would take place mostly in the magmatic arc, where the melt related to the mantle wedge and/or the subducted oceanic lithosphere beneath the obducted ophiolite was originated. However, further geochemical and isotopic studies are required to discuss the metasomatic model in the AR chromitite and the hosting ultramafics.

Variation of Al and Cr contents between massifs of the MG chromitites, on the other hand, is mostly due to either: (1) progressively fractionating parental melts, initially Cr-rich in SSZ (Graham et al., 1996) or (2) melts that originated in different magmatic sources of the ophiolite environment in SSZ regions at different times during the formation and/or evolution of oceanic

lithosphere (Melcher et al., 1997; Ahmed and Arai, 2002; Uysal et al., 2009). Absence of the continuous spectrum of composition of the MG chromitites disagrees with the model of a progressively changing (with time and space) melt composition of one source. In the model of one parent melt of the chromitite ore, it is suggested that the ascending parental melts of chromitites traveled through and were emplaced within a geochemically segmented lithosphere, as suggested by Rollinson (2008) in case of the Oman chromitites. Thus, we propose that the present distribution of Al-richer and Al-poorer chromitites in the small district of Malo Grim most probably reflects temporal and/or spatial variations in the types of melt (boninitic and tholeiitic) that were generated from, and emplaced in, subarc mantle domains in a supra-subduction zone environment.

CONCLUSIONS

Podiform chromitites in the ophiolitic dunite-harzburgite of Arais (AR) and Malo Grim (MG) areas in the southern Eastern Desert of Egypt are of particular interest because they are ones of the few examples where aluminum content varies widely within the same ultramafic massif, over a short distance, and even in the same sample. In massive-textured and big ore bodies chromite survives, showing very little or no alteration; in contrast, chromite from small ore bodies, usually with disseminated texture, is easily altered. However, the metamorphism was slight in the lower greenschist facies (AR) to the transitional greenschist–amphibolite facies (MG). Variation of Al in the unaltered chromian spinel ($Cr\# = 0.57$ to 0.89) estimates island arc low-Ti tholeiitic and boninitic melts for the Al-richer and Al-poorer chromites, respectively. Formation of the high-Cr chromitites took place mostly by reaction of harzburgite with migrating island arc tholeiite melts of boninitic affinity, producing boninitic melts and porous dunitic channels in which the mixing/mingling of melts crystallizing high-Cr chromian spinel. In AR chromitite, the interstitial Al-richer chromite in the Al-poorer one was formed mostly by Al-metasomatism. On the other hand, the Al-compositional variation between massifs of the MG chromitites assumes temporal and/or spatial variations in the types of melt (boninitic and tholeiitic) that were generated from, in the supra-subduction zone.

ACKNOWLEDGEMENTS

We would like to express our deepest gratitude and thanks to Dr. Ryszard Orłowski, ISG-PAS and Dr. P. Dzierzanowski, Faculty of Geology-WU for their help with the EMPA. Logistic support of the Geological Survey and Mining Authority of Egypt during field work is greatly appreciated. Comments of anonymous referees were helpful to improve the manuscript.

REFERENCES

- Abu El Ela AM (1996). Contribution to mineralogy and geochemistry of some serpentinites from the Eastern Desert of Egypt. M.E.R.C. Ain Shams University. *Earth Sci.*, 10: 1-25.
- Abu El Ela FF, Farahat ES (2010). Neoproterozoic podiform chromitites in serpentinites of the Abu Meriewa–Hagar Dungash district, Eastern Desert, Egypt: Geotectonic implications and metamorphism. *Isl. Arc*, 19: 151-164.
- Abu El Laban SA (2002). Some geological and geochemical studies in Abu Ramad Area, South Eastern Desert, Egypt. PhD. Cairo University. p. 274.
- Ahmed AH, Arai S (2002). Unexpectedly high-PGE chromitite from the deeper mantle section of the northern Oman ophiolite and its tectonics implications. *Contrib. Miner. Petr.*, 143: 263-278.
- Ahmed AH, Arai S, Attia AK (2001). Petrological characteristics of podiform chromitites and associated peridotites of the Pan African Proterozoic ophiolite complexes of Egypt. *Miner. Deposita*, 36: 72-84.
- Arai S (1997). Control of wall-rock composition on the formation of podiform chromitites as a result of magma/peridotite interaction. *Resour. Geol.*, 47: 177-187.
- Arai S, Abe N (1994). Possible presence of podiform chromitite in the arc mantle: chromitite xenoliths from the Takashima alkali basalt, southwest Japan arc. *Miner. Deposita.*, 29: 434-438.
- Arai S, Shimizu Y, Ismail SA, Ahmed AH (2006). Low-T formation of high-Cr spinel with apparently primary chemical characteristics within podiform chromitite from Rayat, northeastern Iraq. *Miner. Mag.*, 70: 499-508.
- Arai S, Yurimoto H (1994). Podiform chromitites of the Tari-Misaka ultramafic complex, Southwestern Japan, as mantle–melt interaction products. *Econ. Geol.*, 89: 1279-1288.
- Augé T (1987). Chromite deposits in the northern Oman ophiolite: Mineralogical constraints. *Miner. Deposita.*, 22: 1-10.
- Azer MK, Khalil AE (2005). Petrological and mineralogical studies of Pan-African serpentinites at Bir Al-Edeid area, central Eastern Desert. *Egypt J. Afr. Earth Sci.*, 43: 525-536.
- Azer MK, Stern RJ (2007). Neoproterozoic (835–720 Ma) serpentinites in the Eastern Desert, Egypt: fragments of forearc mantle. *Geology*, 115: 457-472.
- Barnes SJ (2000). Chromite in komatiites, II. Modifications during greenschist to mid-amphibolite facies metamorphism. *J. Petrol.*, 41: 387-409.
- Barnes SJ, Roeder PL (2001). The range of spinel compositions in terrestrial mafic and ultramafic rocks. *J. Petrol.*, 42: 2279-2302.
- Bonavia FF, Diella V, Ferrario A (1993). Precambrian podiform chromitites from Kenticha Hill, southern Ethiopia. *Econ. Geol.*, 88: 198-202.
- Cassard DK, Nicolas AU, Rabinovitch MH, Moutte JD, Leblanc MK, Prinzhofer AG (1981). Structural classification of chromite pods in southern New Caledonia. *Econ. Geol.*, 76: 805-831.
- Dick HJB, Bullen T (1984). Chromian spinel as a petrogenetic indicator in abyssal and alpine-type peridotites and spatially associated lavas. *Contrib. Mineral. Petrol.*, 86: 54-76.
- Droop GTR (1987). A general equation for estimating Fe³⁺ concentrations in ferromagnesian silicates and oxides from microprobe analyses, using stoichiometric criteria. *Mineral. Mag.* 51: 431-435.
- Edwards SJ, Pearce JA, Freeman J (2000). New insights concerning the influence of water during the formation of podiform chromite. In: Dilek Y, Moores EM, Elthon D, Nicolas A. (Eds.), *Ophiolites and oceanic crust: New insights from field studies and the Ocean Drilling Program: Geological Society of America. Special Paper*, 349: 139-147.
- El-Gaby S (2005). Integrated evolution and rock classification of the Pan-African belt in Egypt. First Symposium on the Classification of the Basement Complex of Egypt, pp. 1-9.
- Eliwa HA, Kimura Ji, Itaya T (2006). Late Neoproterozoic Dokhan volcanic rocks, northern Eastern Desert, Egypt. *Precambrian Res.*, 151: 31-52.
- Evans BW, Frost BR (1975). Chrome-spinel in progressive metamorphism - a preliminary analysis. *Geochim. Cosmochim. Ac.*, 39: 959-972.
- Frost BR (1991). Stability of oxide minerals in metamorphic rocks. In: Lindsley, D.H., (Ed.), *Oxide Minerals: Petrologic and Magnetic Significance. Rev. Miner.*, 25: 469-487.
- Fryer P, Taylor B, Langmuir CH, Hochstaedter AG (1990). Petrology and geochemistry of lava from the Sumisu and Torishima backarc rifts. *Earth. Planet. Sci. Lett.*, 100: 161-178.
- Ghoneim MF, Lebda MM, Nasr BB, Khedr MZ (2002). Geology and tectonic evolution of the area around Wadi Arais, Southern Eastern Desert, Egypt. 6th International Conference on the Geology of the Arab World, Cairo University, pp. 45-66.
- González-Jiménez JM, Kerestedjian T, Proenza JA, Gervilla F (2009). Metamorphism on Chromite Ores from the Dobromirski Ultramafic Massif, Rhodope Mountains (SE Bulgaria). *Geol. Ac.*, 7: 413-429.
- González-Jiménez JM, Proenza JA, Gervilla F, Melgarejo JC, Blanco-Moreno JA, Ruiz-Sánchez R, Griffin WL (2011). High-Cr and high-Al chromitites from the Sagua de Tánamo district, Mayarí-Cristal ophiolitic massif (eastern Cuba): Constraints on their origin from mineralogy and geochemistry of chromian spinel and platinum-group elements. *Lithos* doi:10.1016/j.lithos.2011.01.016.
- Graham IT, Franklin BJ, Marshall B (1996). Chemistry and mineralogy of podiform chromitite deposits, southern NSW, Australia: a guide to their origin and evolution. *Miner. Petrol.*, 37: 129-150.
- Grieco G, Ferrario A, Mathez EA (2004). The effect of metasomatism on the Cr-PGE mineralization in the Finero Complex, Ivrea Zone, Southern Alps. *Ore Geol. Rev.*, 24: 299-314.
- Hamdy MM (2007). Stable isotope and trace element characteristics of some serpentinite-hosted vein magnesite deposits from the Eastern Desert of Egypt: arguments for magmatism and metamorphism-related mineralising fluids. M.E.R.C. Ain Shams University. *Earth Sci.*, 21: 29-50.
- Hamdy MM, Harraz HZ, Aly GA (2011). Pan-African (intraplate and subduction-related?) metasomatism in the Fawakhir ophiolitic serpentinites, Central Eastern Desert of Egypt: mineralogical and geochemical evidences. *Arab. J. Geosci. DOI 10.1007/s12517-011-0319-2*.
- Hamdy MM, Lebda EM (2007). Metamorphism of ultramafic rocks at Gebel Arais and Gebel Malo Grim, Eastern Desert, Egypt: mineralogical and O–H stable isotopic constraints. *Egypt J. Geol.*, 51: 105-124.
- Hey MH (1954). A new review of the chlorites. *Mineral. Mag.*, 30: 277-292.
- Johan ZY, Dunlop HH., Le Bel LK, Robert JL, Volfinger MH (1983). Origin of chromite deposits in ophiolitic complexes: Evidence for a volatile- and sodium-rich reducing fluid phase. *Fortschr. Miner.*, 61: 105-107.
- Kamenetsky VS, Crawford AJ, Meffre S (2001). Factors controlling chemistry of magmatic spinel: an empirical study of associated olivine, Cr-spinel and melt inclusions from primitive rocks. *J. Petrol.*, 42: 655-671.
- Kimball KL (1990). Effects of hydrothermal alteration on the composition of chromian spinels. *Contrib. Mineral. Petrol.* 105: 337-346. Lago NL, Rabinowicz M, Nicolas A (1982). Podiform chromite orebodies: a genetic model. *J. Petrol.*, 23: 103-125.
- Kröner A, Greiling RO, Reischmann T, Hussein IM, Stern RJ, Durr S, Kruger J, Zimmer M (1987). Pan-African crustal evolution in the Nubian segment of northeast Africa. In: Kröner A (ed) *Proterozoic lithospheric evolution. American Geophysical Union, Geodynamics Series*, 17: 237-257.
- Leblanc M, Violette JF (1983). Distribution of aluminum-rich and chromium-rich chromite pods in ophiolite peridotites. *Econ. Geol.*, 78: 293-301.
- Matveev S, Ballhaus C (2002). Role of water in the origin of podiform chromitite deposits. *Earth Planet. Sci. Lett.*, 203: 235-243.
- Maurel C, Maurel P (1982). Experimental study of the distribution of aluminum silicate bath between basic and spinel. Petrogenetic implications chromium spinels. *B. Miner.*, 105: 197-202.
- McElduff BF, Stumpfl EF (1991) The chromite deposits of the Troodos complex, Cyprus: Evidence for the role of a fluid phase accompanying chromite formation. *Miner. Deposita*, 26: 307-318.
- Melcher F, Grum W, Simon G, Thalhammer TV, Stumpfl EF (1997). Petrogenesis of the ophiolitic giant chromite deposits of Kempirsai, Kazakhstan: a study of solid and fluid inclusions in chromite. *J.*

- Petrol., 38: 1419-1458.
- Mondal SK, Ripley EM, Li C, Frei R (2006). The genesis of Archaean chromitites from the Nuasahi and Sukinda massifs in the sighbum Craton, India. *Precambrian Res.*, 148: 45-66.
- Mukherjee R, Mondal SK, Rosing MT, Frei R (2010). Compositional variations in the Mesoproterozoic chromitites of the Nuggihalli schist belt, Western Dharwar Craton (India): potential parental melts and implications for tectonic setting. *Contrib. Mineral. Petr.*, 160: 865-885.
- Pearce JA (2003) Subduction zone ophiolites. In: Dilek Y, Newcomb S (eds) *Ophiolite concept and the evolution of geological thought*. *Geol. Soc. Am. Spec. Pap.*, 373: 269-294.
- Peighambari S, Ahmadipour H, Stosch H-G, Daliran F (2011). Evidence for multi-stage mantle metasomatism at the Dehshikh peridotite massif and chromite deposits of the Orzuieh coloured mélange belt, southeastern Iran. *Ore Geol. Rev.*, 39: 245-264.
- Proenza JA, Gervilla F, Melgarejo JC, Bodinier JL (1999). Al- and Cr-rich chromitites from the Mayari-Baracoa Ophiolitic Belt (Eastern Cuba): consequence of interaction between volatile-rich melts and peridotites in suprasubduction mantle. *Econ. Geol.*, 94: 547-566.
- Proenza JA, Ortega-Gutiérrez F, Camprubí A, Tritlla J, Elías-Herrera M, Reyes-Salas M (2004). Paleozoic serpentinite-enclosed chromitites from Tehuiztzingo (Acatlán Complex, southern Mexico): a petrological and mineralogical study. *J. S. Am. Earth Sci.*, 16: 649-666.
- Proenza JA, Zaccarini F, Escayola M, Cávana C, Schalamuk A, Garuti G (2008). Composition and textures of chromite and platinum-group minerals in chromitites of the western ophiolitic belt from Pampean Ranges of Córdoba, Argentina. *Ore Geol. Rev.*, 33: 32-48.
- Roberts S, Neary CR (1993). Petrogenesis of Ophiolitic Chromitite. In: Prichard, H.M., Alabaster, T., Harris, N.B.W., Neary, C.R. (Eds.), *Magmatic Processes and Plate Tectonics*: Geological Society of London, Special Publication, 76: 257-272.
- Roeder PL, Reynolds I (1991). Crystallization of chromite and chromium solubility in basaltic melts. *J. Petrol.*, 32: 909-934.
- Rollinson H (1995). Composition and tectonic settings of chromite deposits through time—a discussion. *Econ. Geol.*, 90: 2091-2098.
- Rollinson H (2005). Chromite in the mantle section of the Oman ophiolite: a new genetic model. *Isl. Arc*, 14: 542-550.
- Rollinson H (2008). The geochemistry of mantle chromitites from the northern part of the Oman ophiolite: inferred parental melt compositions. *Contrib. Mineral. Petr.*, 156: 273-288.
- Saleh GM (2006). The chromite deposits associated with ophiolite complexes, Southeastern Desert, Egypt: Petrological and geochemical characteristics and mineralization. *Chinese J. Geochem.*, 25: 307-317.
- Schiano P, Clocchiatti R, Lorand JP, Massare D, Deloule E, Chaussidon M (1997). Primitive basaltic melts included in podiform chromites from the Oman ophiolite. *Earth Planet. Sci. Lett.*, 146: 489-497.
- Scowen PAH, Roeder PL, Helz RT (1991). Re-equilibration of chromite within Kilauea Iki lava lake, Hawaii. *Contrib. Mineral. Petr.*, 107: 8-20.
- Shervais JW, Kimbrough DL, Renne PR, Hanan BB, Murckey B, Snow CA, Schuman MMZ, Beaman J (2004). Multi-stage origin of the Coast Range ophiolite, California: implications for the life cycle of supra-subduction zone ophiolites. *Int. Geol. Rev.*, 46: 289-315.
- Stern RJ (1994). Arc assembly and continental collision in the Neoproterozoic East African Orogen: implications for the consolidation of Gondwanaland. *Annu. Rev. Earth Planet. Sci.*, 22: 319-351.
- Stern RJ, Johanson PR, Kroner A, Yibas B (2004). Neoproterozoic ophiolites of the Arabian-Nubian Shield. In: Kusky TM (ed) *Precambrian ophiolites and related rocks*. *Developments in Precambrian Geology*, Elsevier, Amsterdam, 13: 95-128.
- Suita MT, Streider AJ (1996). Cr-spinels from Brazilian mafic-ultramafic complexes: metamorphic modifications. *Int. Geol. Rev.* 38: 245-267.
- Uysal I, Tarkian M, Sadiklar MB, Zaccarini F, Meisel T, Garuti G, Heidrich S (2009). Petrology of Al- and Cr-rich ophiolitic chromitites from the Muğla, SW Turkey: implications from composition of chromite, solid inclusions of platinum group mineral, silicate, and base-metal mineral, and Os-isotope geochemistry. *Contrib. Mineral. Petr.*, 158: 659-674.
- Wilson M (1989). *Igneous Petrogenesis, a Global Tectonic Approach*. Chapman and Hall, London.
- Zhou MF, Robinson PT (1994). High-Cr and high-Al podiform chromitites, Western China: relationships to partial melting and melt/rock reaction in the upper mantle. *Int. Geol. Rev.*, 36: 678-686.
- Zhou MF, Robinson PT (1997). Origin and tectonic environment of podiform chromite deposits. *Econ. Geol.*, 92: 259-262.
- Zhou MF, Robinson PT, Malpas J, Aitchison J, Sun M, Bai WJ, Hu XF, Yang JS (2001). Melt/mantle interaction and melts evolution in the Sartohay high-Al chromite deposits of the Salabute ophiolite (NW China). *J. Asian Earth Sci.*, 19: 517-534.
- Zhou MF, Robinson PT, Malpas J, Zijin L (1996). Podiform chromites in the Luobusa Ophiolite (Southern Tibet): implications for melt-rock interaction and chromite segregation in the upper mantle. *J. Petrol.*, 37: 3-21.